Available online at www.sciencedirect.com
SCIENCE DIRECT®
Journal of Sound and Vibration 289 (2006) 264–277
JOURNAL OF SOUND AND VIBRATION
www.elsevier.com/locate/jsvi

Postbuckling and vibration of end-supported elastica pipes conveying fluid and columns under follower loads

R.H. Plaut*

The Charles E. Via, Jr. Department of Civil and Environmental Engineering, Virginia Polytechnic Institute and State University, Blacksburg, VA 24061-0105, USA

Received 26 July 2004; received in revised form 24 January 2005; accepted 5 February 2005
Available online 12 May 2005

Abstract

Fluid-conveying pipes with supported ends buckle when the fluid velocity reaches a critical value. For higher velocities, the postbuckled equilibrium shape can be directly related to that for a column under a follower end load. However, the corresponding vibration frequencies are different due to the Coriolis force associated with the fluid flow. Clamped–clamped, pinned–pinned, and clamped–pinned pipes are considered first. Axial sliding is permitted at the downstream end. The pipe is modeled as an inextensible elastica. The equilibrium shape may have large displacements, and small motions about that shape are analyzed. The behavior is conservative in the prebuckling range and nonconservative in the postbuckling range (during which the Coriolis force does work and the motions decay). Next, related columns are studied, first with a concentrated follower load at the axially sliding end, and then with a distributed follower load. In all cases, a shooting method is used to solve the nonlinear boundary-value problem for the equilibrium configuration, and to solve the linear boundary-value problem for the first four vibration frequencies. The results for the three different types of loading are compared.

1. Introduction

The behavior of fluid-conveying pipes has been studied extensively [1,2]. In general, both static instability (buckling) and dynamic instability (flutter) may occur. If the ends of a single-span pipe

*Tel.: +1 540 231 6072; fax: +1 540 231 7532.
E-mail address: rplaut@vt.edu.

0022-460X/$ - see front matter © 2005 Elsevier Ltd. All rights reserved.
doi:10.1016/j.jsv.2005.02.032

are either clamped or pinned, buckling occurs at a critical value of the fluid velocity. The fundamental frequency of vibration for small motions about the straight pipe becomes zero at the critical velocity. As the velocity is increased above its critical value, the pipe takes on postbuckled equilibrium shapes with ever-increasing displacements.

Prebuckling vibrations of end-supported pipes, as a function of the fluid velocity, have been investigated theoretically and experimentally in a number of studies, including Refs. [1–10]. Sorokin and Terentiev [11] considered a pinned–pinned pipe which was buckled by an axial force or deflected by two applied moments, and then subjected to a fluid flow which did not affect the equilibrium shape of the pipe. Small vibrations about equilibrium were investigated.

Postbuckling of pipes with immovable ends was investigated by Holmes [12] and others. Deflections can become large if one end of the pipe is allowed to slide axially. Equilibrium shapes for such cases were described in Refs. [13–15] using an elastica analysis for the pipe. In Ref. [15], vibrations also were examined. The pipe was hung at the bottom of a tank which contained water at constant height. The top of the pipe was clamped and the bottom was pinned. In the analysis, the weights of the pipe and fluid were included. The fluid velocity in the pipe was an unknown function of time. Analytical and experimental results were presented.

Small vibrations about postbuckled equilibrium configurations are analyzed here. Each end of the pipe is either clamped or pinned, and the downstream end is free to move in the axial direction, as depicted in Fig. 1. Damping and gravitational effects are neglected. Results for free vibrations about the straight pipe, when the velocity is less than the critical value, are obtained first. These frequencies can be used in practice to predict the critical velocity by extrapolation from a few results at low velocities [16].

For fluid velocities above the critical value, the equilibrium shapes (which may involve large displacements) are determined, and the first four frequencies for small vibrations about these configurations are computed. The corresponding motions decay with time. As the velocity increases, the frequencies do not necessarily change in a monotonic manner. The problem is formulated in Section 2, and numerical results are presented in Section 3.

Next, related columns subjected to follower loads are treated using the same type of formulation and solution procedure. Much attention has been given to cantilevered columns which exhibit dynamic instability (flutter) under sufficiently large follower loads [17]. If the ends are supported, initial instability is caused by buckling (divergence), as for pipes [18]. The postbuckling deflections, and small vibrations about the equilibrium configurations, are examined here for a follower end load (Section 4) and a distributed follower load (Section 5). For the first of these cases, the postbuckled equilibrium shape is the same as for the associated pipe, and the frequencies can be compared directly. Finally, concluding remarks are given in Section 6.

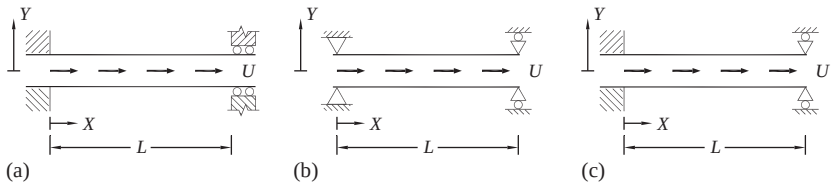

Fig. 1. Geometry of pipe. (a) clamped–clamped; (b) pinned–pinned; (c) clamped–pinned.

2. Formulation for pipe

The pipe is assumed to be an elastica, which is thin, flexible, inextensible, and unshearable, with bending moment proportional to curvature. Its thickness is assumed to be small relative to its diameter, which is small relative to the length. The pipe is uniform with constant bending stiffness EI, constant mass per unit length μ_p, and length L. The fluid has constant velocity U and constant mass per unit length μ_f, and its profile is uniform (i.e., plug flow is assumed [2]). Damping and the weights of the pipe and fluid are neglected. Planar motion is considered.

From the left end in Fig. 1, the arc length is S, the axial and transverse coordinates are $X(S,T)$ and $Y(S,T)$, respectively, and the rotation angle in radians is $\theta(S,T)$, where T denotes time. The bending moment $M(S,T)$ is positive if it tends to produce positive curvature. The horizontal force in the column is denoted $P(S,T)$ and is positive if it is compressive. The vertical force is $Q(S,T)$ and is positive if downward on a positive face (i.e., if it tends to rotate the pipe clockwise). Dimensional vibration frequencies are denoted Ω.

Based on geometry, moment–curvature relationship, and dynamic equilibrium, the governing equations are as follows [13,14,19]:

$$\begin{aligned} &X_S = \cos\theta, \quad Y_S = \sin\theta, \quad EI\theta_S = M, \quad M_S = Q\cos\theta - P\sin\theta,\\ &P_S = -(\mu_f+\mu_p)X_{TT} - 2\mu_f U X_{ST} - \mu_f U^2 X_{SS},\\ &Q_S = -(\mu_f+\mu_p)Y_{TT} - 2\mu_f U Y_{ST} - \mu_f U^2 Y_{SS}, \end{aligned} \tag{1}$$

where subscripts S and T denote partial derivatives.

The analysis is carried out in terms of the nondimensional quantities

$$\begin{aligned} &x = \frac{X}{L}, \quad y = \frac{Y}{L}, \quad s = \frac{S}{L}, \quad m = \frac{ML}{EI}, \quad p = \frac{PL^2}{EI},\\ &q = \frac{QL^2}{EI}, \quad t = \frac{T}{L^2}\sqrt{\frac{EI}{\mu_f+\mu_p}}, \quad \omega = \Omega L^2\sqrt{\frac{\mu_f+\mu_p}{EI}},\\ &u = UL\sqrt{\frac{\mu_f}{EI}}, \quad \beta = \frac{\mu_f}{\mu_f+\mu_p}. \end{aligned} \tag{2}$$

In nondimensional terms, the governing equations are

$$\begin{aligned} &x_s = \cos\theta, \quad y_s = \sin\theta, \quad \theta_s = m, \quad m_s = q\cos\theta - p\sin\theta,\\ &p_s = -x_{tt} - 2\sqrt{\beta}u x_{st} - u^2 x_{ss}, \quad q_s = -y_{tt} - 2\sqrt{\beta}u y_{st} - u^2 y_{ss}. \end{aligned} \tag{3a–f}$$

The subscript e denotes quantities associated with the equilibrium state, and the subscript d is used for dynamic quantities related to small free motions about equilibrium. The variables are written in the following complex form:

$$\begin{aligned} &x(s,t) = x_e(s) + x_d(s)e^{i\omega t}, \quad y(s,t) = y_e(s) + y_d(s)e^{i\omega t},\\ &\theta(s,t) = \theta_e(s) + \theta_d(s)e^{i\omega t}, \quad m(s,t) = m_e(s) + m_d(s)e^{i\omega t},\\ &p(s,t) = p_e(s) + p_d(s)e^{i\omega t}, \quad q(s,t) = q_e(s) + q_d(s)e^{i\omega t}. \end{aligned} \tag{4}$$

With the use of Eq. (4) in Eqs. (3a–f), the governing equations for equilibrium are found to be

$$x_e' = \cos\theta_e, \quad y_e' = \sin\theta_e, \quad \theta_e' = m_e,$$
$$m_e' = q_e\cos\theta_e - p_e\sin\theta_e, \quad p_e' = -u^2x_e'', \quad q_e' = -u^2y_e'' \tag{5a–f}$$

and the governing linear dynamic equations are given by

$$x_d' = -\theta_d\sin\theta_e, \quad y_d' = \theta_d\cos\theta_e, \quad \theta_d' = m_d,$$
$$m_d' = (q_d - p_e\theta_d)\cos\theta_e - (p_d + q_e\theta_d)\sin\theta_e,$$
$$p_d' = \omega^2x_d - 2\mathrm{i}\sqrt{\beta}u\omega x_d' - u^2x_d'',$$
$$q_d' = \omega^2y_d - 2\mathrm{i}\sqrt{\beta}u\omega y_d' - u^2y_d''. \tag{6a–f}$$

If Eqs. (5e,f) are integrated and Eqs. (5a,b) are used, one obtains

$$p_e = p_o - u^2\cos\theta_e, \quad q_e = q_o - u^2\sin\theta_e, \tag{7a,b}$$

where p_o and q_o are constants. Substituting Eqs. (7a,b) into Eq. (5d) yields

$$m_e' = q_o\cos\theta_e - p_o\sin\theta_e. \tag{8}$$

Eqs. (7a,b) are used in Eq. (6d). Also, Eqs. (6a,b) and their derivatives are substituted into Eqs. (6e,f). This results in

$$m_d' = (q_d - p_o\theta_d)\cos\theta_e - (p_d + q_o\theta_d)\sin\theta_e + u^2\theta_d,$$
$$p_d' = \omega^2x_d - (2\mathrm{i}\sqrt{\beta}u\omega\theta_d + u^2m_d)\sin\theta_e + u^2m_e\theta_d\cos\theta_e,$$
$$q_d' = \omega^2y_d - (2\mathrm{i}\sqrt{\beta}u\omega\theta_d + u^2m_d)\cos\theta_e + u^2m_e\theta_d\sin\theta_e. \tag{9}$$

If the left end $s = 0$ is clamped, the boundary conditions there are $x_e = y_e = \theta_e = x_d = y_d = \theta_d = 0$. If it is pinned, $x_e = y_e = m_e = x_d = y_d = m_d = 0$. Axial sliding is permitted at the end $s = 1$. If that end is clamped, $y_e = \theta_e = p_e = y_d = \theta_d = p_d = 0$ there. If it is pinned, $y_e = m_e = p_e = y_d = m_d = p_d = 0$. Based on Eq. (7a), the boundary condition $p_e(1) = 0$ can be replaced by $u^2\cos\theta_e(1) = p_o$.

In nondimensional terms, the sum H of the kinetic energy and strain energy is

$$H = \frac{1}{2}\int_0^1 (x_t^2 + y_t^2 + \theta_s^2)\,\mathrm{d}s. \tag{10}$$

The time rate of change of H can be put in the form

$$\frac{\mathrm{d}H}{\mathrm{d}t} = -u\sqrt{\beta}[x_t(1,t)]^2 - u^2x_t(1,t)\cos\theta(1,t) \tag{11}$$

by making use of Eqs. (3a–f), the derivatives of Eqs. (3a,b), and the boundary conditions. On the right-hand side of Eq. (11), the first term (which is negative) represents the rate of work done by the Coriolis force; it is proportional to the fluid velocity, the square root of the mass ratio parameter, and the square of the axial velocity of the pipe at the sliding end. The second term corresponds to the centrifugal force, and for the clamped–clamped pipe it is the time derivative of $-u^2x(1,t)$. For motions about the postbuckled equilibrium configuration, the system is not

conservative, and in the numerical results the associated values of ω are complex with positive imaginary part, so that the motions about the postbuckled states decay with time.

3. Numerical results for pipe

The critical fluid velocities for the clamped–clamped, pinned–pinned, and clamped–pinned pipes are $u_{CR} = 2\pi$, π, and 4.493, respectively. Postbuckled equilibrium shapes for higher values of velocity are obtained from Eqs. (5a–c) and (8). These first-order equations are solved numerically using a shooting method with the subroutines NDSolve and FindRoot in Mathematica [20]. For the clamped–pinned pipe, q_o is specified, and p_o and $m_e(0)$ are varied until $y_e(1) = m_e(1) = 0$ with sufficient accuracy; then u is obtained from $u^2 \cos\theta_e(1) = p_o$. For the clamped–clamped and pinned–pinned cases, the equilibrium shapes are symmetric about $s = 0.5$, and $q_o = 0$, so there is one less unknown parameter to be varied.

The maximum value of $y_e(s)$ is denoted y_{max}, which occurs at $s = 0.5$ for the clamped–clamped and pinned–pinned cases. Curves of u vs y_{max} are presented in Fig. 2, along with some associated equilibrium shapes. The solid curve for the clamped–clamped pipe is stopped when the left and right parts of the pipe contact each other, which occurs when $u = 8.50$ and $y_{max} = 0.403$ [21]. The shape of the pipe at this stage is shown in Fig. 2. The other clamped–clamped shapes correspond to $(u,\ y_{max}) = (6.4, 0.167)$ and (6.8, 0.309). For the dashed and dotted curves, the velocity u approaches infinity as the magnitude of the pipe rotation θ_e at $s = 1$ approaches $\pi/2$. This occurs as y_{max} approaches 0.31 for the clamped–pinned pipe and 0.38 for the pinned–pinned case. The equilibrium shapes depicted with these curves correspond to $(u, y_{max}) = (5.7, 0.202)$ and (4.0, 0.246), respectively, for the clamped–pinned and pinned–pinned pipes.

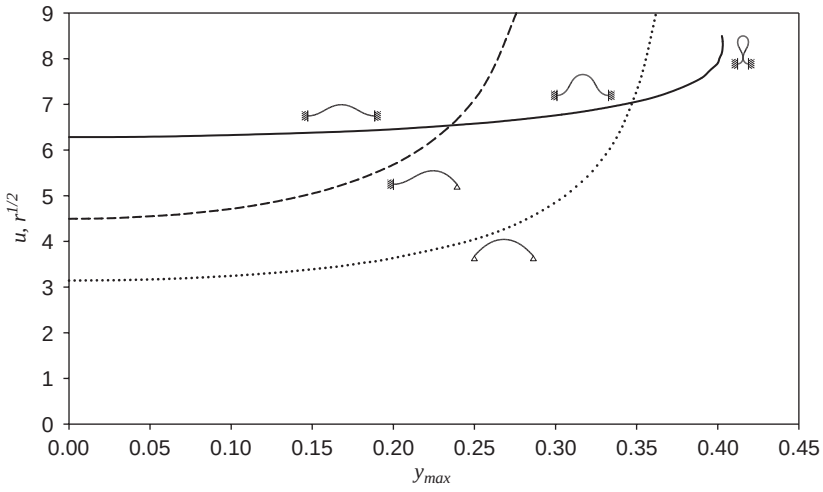

Fig. 2. Equilibrium paths for pipe (velocity vs maximum deflection) and column with end follower load (square root of load vs maximum deflection) in nondimensional terms. ———, clamped–clamped; ....., pinned–pinned; - - - -, clamped–pinned.

To determine vibration frequencies, Eqs. (6a–c) and (9) are solved numerically. These equations are linear in the dynamic variables, but their coefficients are functions of s and are not known analytically. Results from the equilibrium solution are utilized, i.e., values of u, p_o, q_o, and either $\theta_e(0)$ or $m_e(0)$. Since the amplitude of the free vibration is arbitrary, the value of one of the dynamic variables at $s = 0$ is specified (e.g., $q_d(0) = 0.1$). The other two unknown values of variables at $s = 0$, and the frequency ω, are varied until the three conditions at $s = 1$ are satisfied. By guessing the value of ω in different ranges, frequencies corresponding to different modes can be computed.

First, prebuckling vibrations are analyzed ($0 < u < u_{CR}$). The pipe is straight, so that $\theta_e(s) = 0$. In this prebuckling range, the values of the nondimensional frequency ω are real. Due to the Coriolis force, the pipe does not exhibit classical modes. When it vibrates at one of the vibration frequencies, the shape changes with time [1,2].

For the mass ratio parameter $\beta = 0.5$, the first four frequencies ω or their real parts (if ω is complex) are plotted as solid curves in Figs. 3–5 for the three sets of boundary conditions, respectively. In the prebuckling range, the frequencies decrease as the velocity increases, and the fundamental frequency is zero when $u = u_{CR}$ (denoted by a dotted horizontal line). In this range, if u^2 were plotted vs ω^2, the curves would be almost linear.

For postbuckling, small vibrations about the nontrivial equilibrium configuration are examined. The lowest four real parts of the solutions ω, corresponding to the oscillatory part of the motion for each of these modes, are plotted in Figs. 3–5. These real parts will be called the frequencies.

As the velocity increases beyond its critical value, the frequencies do not behave monotonically. In Fig. 3 (clamped–clamped pipe), the fundamental frequency increases in the range shown, the second frequency increases and then decreases, and the third and fourth frequencies decrease significantly and then increase. For the pinned–pinned case in Fig. 4, the first frequency increases and then decreases, the second frequency decreases, increases, and then decreases, and again the

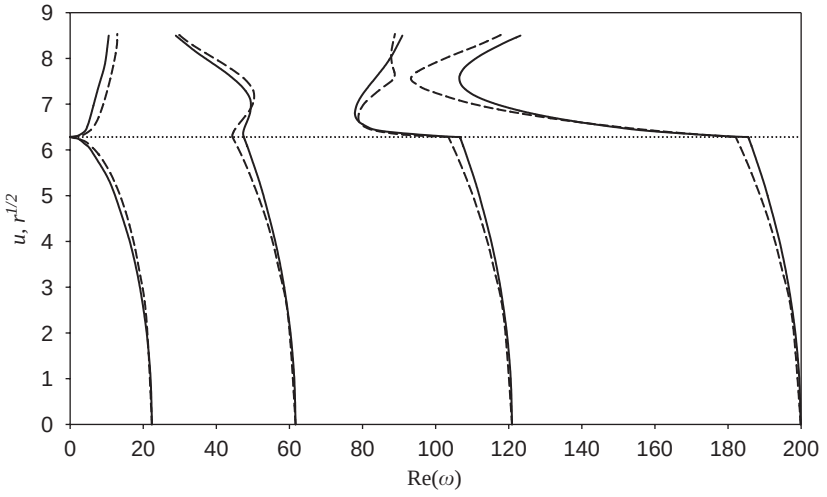

Fig. 3. Vibration frequencies for clamped–clamped boundary conditions. ——, u for pipe ($\beta = 0.5$); - - - - -, $r^{1/2}$ for column with end follower load.

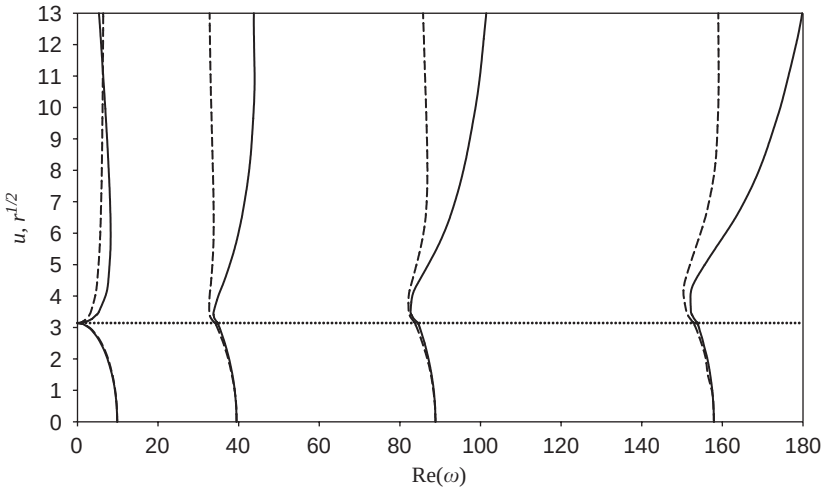

Fig. 4. Vibration frequencies for pinned–pinned boundary conditions. ——, u for pipe ($\beta = 0.5$); - - - - -, $r^{1/2}$ for column with end follower load.

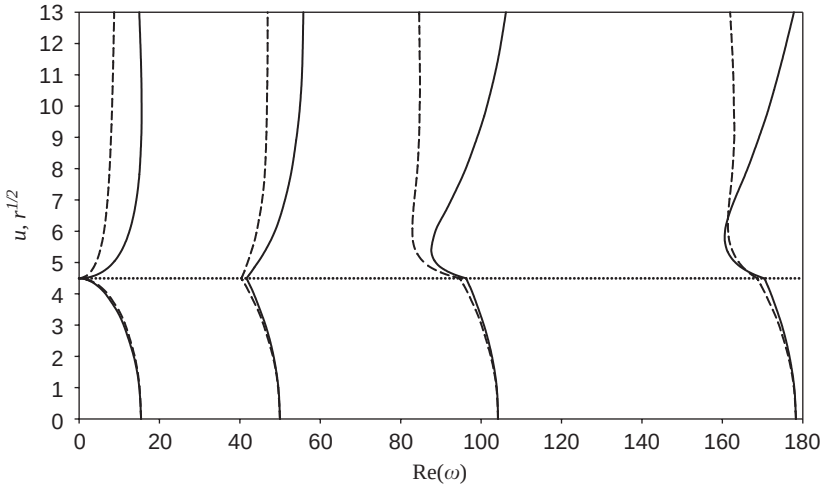

Fig. 5. Vibration frequencies for clamped–pinned boundary conditions. ——, u for pipe ($\beta = 0.5$); - - - - -, $r^{1/2}$ for column with end follower load.

third and fourth frequencies decrease and then increase. In Fig. 5 (clamped–pinned pipe), the first frequency increases and then decreases, the second frequency increases in the range shown, and the third and fourth frequencies decrease and then increase.

The imaginary parts of ω represent the rates of decay of the modes following a perturbation from the buckled equilibrium state. As the velocity increases past the critical value, the rates increase from zero. The decay rate is larger for the first mode than for any of the next three modes until u reaches 7.4, 5.0, and 22.2 for the clamped–clamped, pinned–pinned, and clamped–pinned pipes, respectively, and the corresponding values of the imaginary part of ω are 5.8, 4.0, and 15.5.

The value of the mass ratio parameter β affects the frequencies. For vibrations about a buckled state, the first frequency decreases as β increases. However, higher frequencies sometimes decrease and sometimes increase as β is increased.

4. End-supported columns with follower end load

Thompson and Lunn [13] showed that the postbuckled equilibrium shapes for the pipes in Fig. 1 are the same as for a column with the same boundary conditions and subjected to a follower load $R = \mu_f U^2$. The case of clamped–pinned boundary conditions is sketched in Fig. 6(a). Axial sliding is permitted at the loaded support. In nondimensional terms, the load is

$$r = RL^2/EI \tag{12}$$

and correlates with u^2 for the pipe. It is interesting to compare the vibration frequencies for small motions about the same equilibrium shape (as well as vibrations about the prebuckled straight equilibrium configuration).

Eqs. (3)–(9) are valid here if u is set equal to zero. The boundary conditions are the same as for the pipe except that the conditions $p_e = p_d = 0$ at $s = 1$ are replaced by $p_e = r\cos\theta_e$ and $p_d = -r\theta_d \sin\theta_e$. If H is defined by Eq. (10), its rate of change is given by Eq. (11) if β is set equal to zero and u^2 is replaced by r. For the clamped–clamped column, the rate of change of $H + rx(1,t)$ is zero and the system is conservative.

For these columns with follower end loads, the equilibrium paths in Fig. 2 are valid if the ordinate is taken as $r^{1/2}$. (In the clamped–clamped case, the end load remains parallel to the x-axis and does not change direction.) The frequencies are not equal to those for the pipe, due to the Coriolis force acting on the pipe. Here, the frequencies are real under both prebuckling and postbuckling conditions. Numerical results are shown by the dashed lines in Figs. 3–5, with the ordinate being $r^{1/2}$.

For the clamped–clamped case (Fig. 3), the first frequency is higher than that for the pipe except at low loads. The other three frequencies are lower for most of the prebuckling range and at least part of the postbuckling range, after which the second and third frequencies become higher and then the third becomes lower again shortly before self-contact occurs.

For the pinned–pinned case (Fig. 4), the frequencies for the end load and the pipe are almost the same under prebuckling conditions. For vibrations about the postbuckled equilibrium state, the corresponding column frequencies are lower except for the fundamental frequency when the load becomes very large. For the clamped–pinned case (Fig. 5), again the prebuckling frequencies are similar, and for postbuckling, the first three frequencies are lower for the column in the range shown, and the fourth frequency becomes significantly lower for sufficiently high loads.

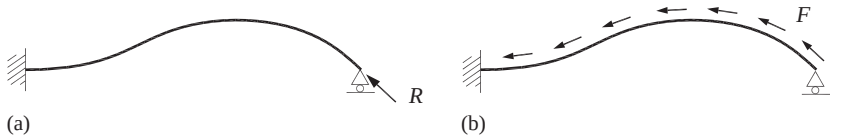

Fig. 6. Geometry of column. (a) end follower load; (b) distributed follower load.

5. End-supported columns with distributed follower load

Columns with distributed follower loads have been qualitatively related to pipes conveying fluid. Fig. 6(b) shows the clamped–pinned case with constant distributed compressive follower load F per unit length. The nondimensional load is defined by

$$f = FL^3/EI \tag{13}$$

and critical loads for clamped–clamped, pinned–pinned, and clamped–pinned boundary conditions are 80.26, 18.96, and 57.01, respectively [18]. An elastica formulation for equilibrium of the pinned–pinned case (Pflüger's column) was presented by Atanackovic and Simic [22], but no postbuckling conditions were considered.

Eqs. (3a–d), (4), (5a–d), and (6a–d) still apply, and Eqs. (3e,f), (5e,f), and 6(e,f) are replaced by the following:

$$p_s = -x_{tt} - f\cos\theta, \quad q_s = -y_{tt} - f\sin\theta, \tag{14}$$

$$p'_e = -f\cos\theta_e, \quad q'_e = -f\sin\theta_e, \tag{15}$$

$$p'_d = \omega^2 x_d + f\theta_d\sin\theta_e, \quad q'_d = \omega^2 y_d - f\theta_d\cos\theta_e. \tag{16}$$

The boundary conditions are the same as for the pipe, with axial sliding allowed at $s = 1$. Making use of Eqs. (3a,b), integration of Eq. (15), and the boundary condition $p_e(1) = 0$, one can obtain

$$p_e = p_o - fx_e, \quad q_e = q_o - fy_e, \quad p_o = fx_e(1). \tag{17}$$

With H given by Eq. (10), its rate of change is

$$\frac{\mathrm{d}H}{\mathrm{d}t} = -f\int_0^1 (x_t\cos\theta + y_t\sin\theta)\,\mathrm{d}s. \tag{18}$$

Equilibrium paths are plotted in Fig. 7 for $0<f<150$. The equilibrium shapes shown for the clamped–clamped (solid curve) and clamped–pinned (dashed curve) columns correspond to $(f, y_{\max}) = (129.4, 0.302)$ and (105.2, 0.279), respectively. For the pinned–pinned column (dotted curve), the postbuckling path starts at the critical load $f = 18.96$ and rises until it reaches a limit (maximum) point at $f = 36.1$. Then it turns around, and the curve is continued until $f = 0$. The equilibrium shape on the initial part of the path corresponds to $(f, y_{\max}) = (23.8, 0.245)$, the next one is at the limit point $(f, y_{\max}) = (36.1, 0.372)$, the third shape is at the point $(f, y_{\max}) = (19.5, 0.290)$ for which the column is tangential to the x-axis (i.e., $\theta_e = \pi$) at $s = 0$, and the final shape (which is symmetric with respect to the x-axis) is at $f = 0$ and $y_{\max} = 0.129$.

The equilibrium states between the limit point and the final point at $f = 0$ are unstable. As the load f is increased from zero, a smooth transition to stable nontrivial equilibrium states occurs as f passes 18.96. The transverse deflection increases until $f = 36.1$, and if the load is increased further, the column experiences a sudden collapse. This type of equilibrium path, with a bifurcation point followed by a limit point, is unusual. More common is secondary bifurcation, in which a postbuckled equilibrium path becomes unstable when it is intersected by another path [23].

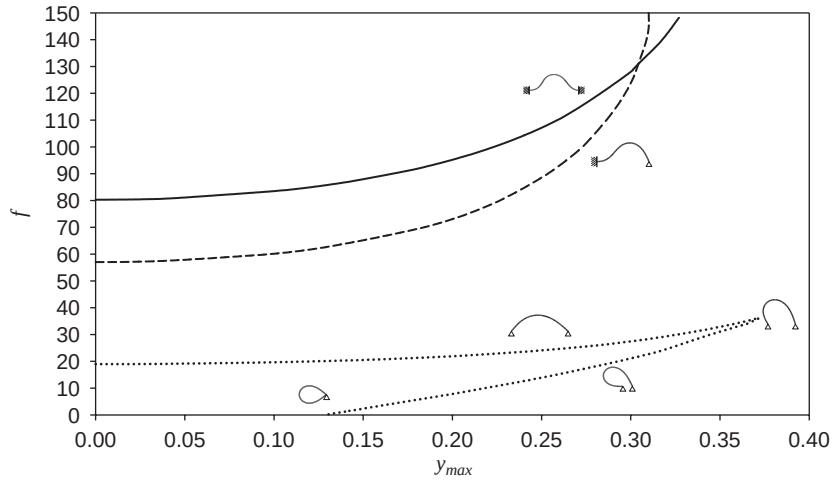

Fig. 7. Equilibrium paths (load vs maximum deflection) for end follower load in nondimensional terms. ———, clamped–clamped; ....., pinned–pinned; - - - -, clamped–pinned.

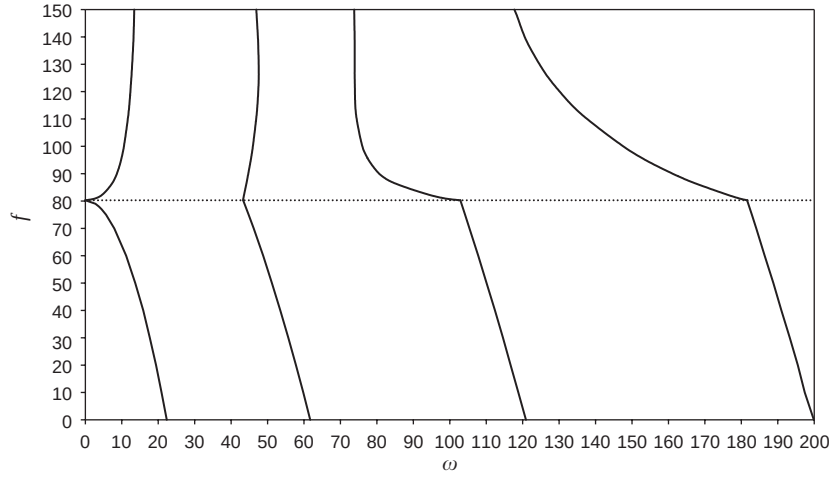

Fig. 8. Load vs vibration frequency for clamped–clamped column with distributed follower load.

The vibration frequencies are real for small motions about the stable equilibrium states. The first four frequencies are plotted in Figs. 8–10 for the clamped–clamped, pinned–pinned, and clamped–pinned columns, respectively. After the critical load is reached (dotted line), initially the first two frequencies increase and the next two frequencies decrease, except for the second frequency in Fig. 9. For the pinned–pinned column (Fig. 9), the fundamental frequency decreases to zero at the limit point, as it must, and the curves are not continued further since the column collapses. Corresponding to the unstable equilibrium states in Fig. 7, the fundamental mode would exhibit an exponentially growing motion (i.e., ω is an imaginary number in the solution of the linear vibration problem).

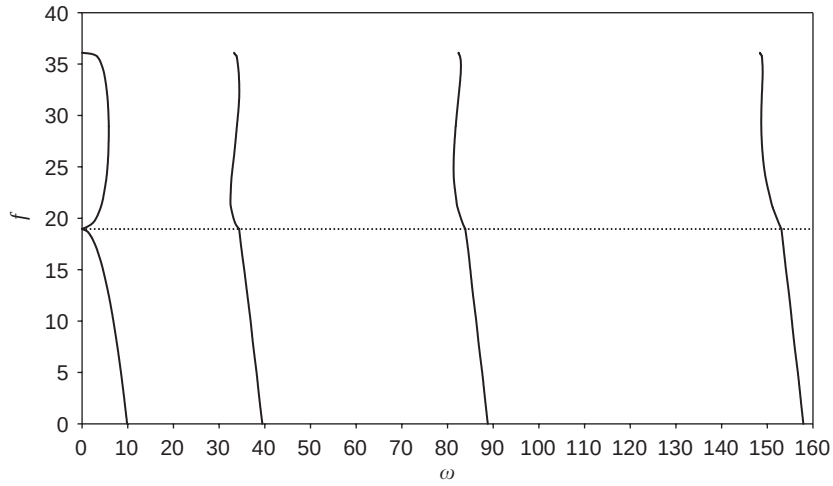

Fig. 9. Load vs vibration frequency for pinned–pinned column with distributed follower load.

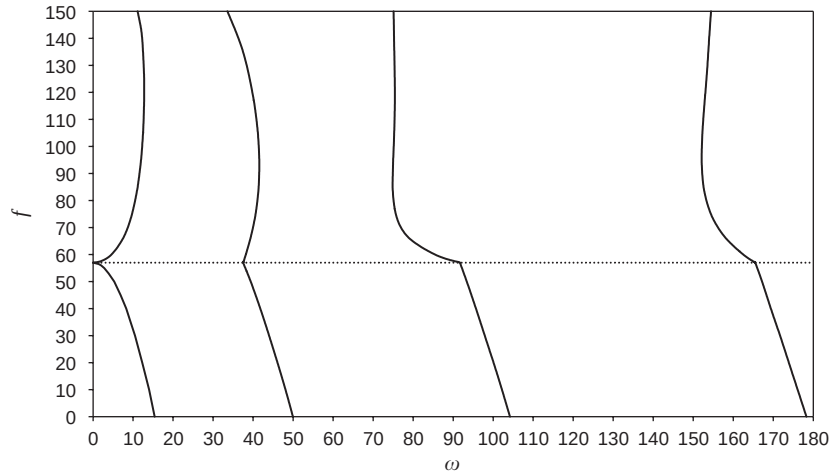

Fig. 10. Load vs vibration frequency for clamped–pinned column with distributed follower load.

6. Concluding remarks

Postbuckling and vibrations were investigated for pipes and columns with ends that do not deflect transversely. Axial sliding was permitted at one end. It was assumed that deflections occur in a plane. Each pipe and column was modeled as an inextensible elastica. This allows large displacements in equilibrium, and makes it easy to include both transverse and axial inertia forces in the governing equations, and to treat the axial boundary condition at the sliding end. (Extensibility and a nonlinear moment–curvature relation could easily be added to the formulation [24,25].) It was assumed that the cross-section does not change during deflection.

Numerical solutions were obtained with the use of a shooting method, in which the boundary-value problem was treated as an initial value problem. First the equilibrium shape was obtained, and then small vibrations about this configuration were analyzed.

For the pipe, the fluid velocity was assumed to be constant (which may not be realistic in some physical situations, especially at high velocities). Periodic motion (but not classical normal modes) can occur if the fluid velocity is less than its critical value (i.e., under prebuckling conditions, when the equilibrium configuration of the pipe is straight). For free vibrations about the postbuckled equilibrium states, the motion decays. This is due to the Coriolis force and sometimes the centrifugal force, in conjunction with axial sliding at the downstream end; no damping is assumed in the analysis. The frequency of the oscillatory part of the motion was computed for the first four modes with the mass ratio parameter set at $\beta = 0.5$. In the range $0<\beta<1$, if β increases, the nondimensional fundamental frequency decreases (as shown in Ref. [1] for the pinned–pinned pipe and $0<u<u_{CR}$), whereas the higher nondimensional frequencies may either decrease or increase.

One can define the ''corresponding nongyroscopic system'' to the pipe as that system for which the Coriolis term is not included (i.e., $\beta = 0$). This system corresponds to a column subjected to an axial end load. At any velocity below the critical one, the computed fundamental frequency for the pipe in the cases treated here is always lower than that for the corresponding nongyroscopic system. This is consistent with a general result for discretized systems [26,27], and the corresponding nongyroscopic system can be used to obtain an upper bound on the prebuckled fundamental frequency.

For the corresponding column subjected to a compressive follower load at the axially sliding end, the postbuckled equilibrium shapes are the same as those for the pipe with fluid velocity related to the square root of the load. Vibration frequencies for the two systems do not correlate directly, due to the Coriolis force acting on the pipe, and in the postbuckled range the frequencies may be quite different for the pipe and the column with follower end load.

The corresponding columns subjected to a uniformly distributed follower load were also analyzed. Motions about the prebuckled and postbuckled equilibrium states do not decay for the follower-load problems treated here. An interesting result is that the postbuckled equilibrium configuration for the pinned–pinned case with distributed load (Pflüger's column) becomes unstable at a limit point when the load reaches a certain magnitude, and the column then collapses.

If small damping were added to the formulations here, the frequencies would not change drastically. There is no sudden ''destabilization'' of a stable equilibrium state, as may occur for a nonconservative system which exhibits dynamic instability [2,17], such as a cantilevered fluid-conveying pipe or a cantilevered column subjected to a compressive follower load.

Variation of the fundamental vibration frequency as a function of velocity or load can be utilized to predict the critical (buckling) condition. If the fundamental frequency can be measured at a few velocities or loads, then these values can be extrapolated to obtain an estimate or upper bound for the critical velocity or load. This technique can be improved by plotting the load or the square of the velocity as a function of the square of the fundamental frequency, so that the curve is almost linear.

Potential applications of this work to highly flexible pipes and hoses are described in Ref. [2]. They include mass-flow meters, vibration-attenuation devices, and deep-water risers.

Acknowledgements

This research was supported by the US National Science Foundation under Grant No. CMS-0301084. The author is grateful to the reviewers for their helpful comments.

References

[1] S.-S. Chen, *Flow-Induced Vibration of Circular Cylindrical Structures*, Hemisphere, Washington, DC, 1987.
[2] M.P. Païdoussis, *Fluid–Structure Interactions*: *Slender Structures and Axial Flow*, vol. 1, Academic Press, San Diego, CA, 1998.
[3] R.H. Long Jr., Experimental and theoretical study of transverse vibration of a tube containing flowing fluid, *Journal of Applied Mechanics* 22 (1955) 65–68.
[4] H.L. Dodds Jr., H.L. Runyan, Effect of high velocity fluid flow on the bending vibrations and static divergence of a simply supported pipe, NASA Technical Note D-2870, 1965.
[5] S. Naguleswaran, C.J.H. Williams, Lateral vibrations of a pipe conveying fluid, *Journal of Mechanical Engineering Science* 10 (1968) 228–238.
[6] S.S. Chen, G.S. Rosenberg, Vibrations and stability of a tube conveying fluid, Argonne National Laboratory Report ANL-7762, 1971.
[7] H.-S. Liu, C.D. Mote Jr., Dynamic response of pipes transporting fluids, *Journal of Engineering for Industry* 96 (1974) 591–596.
[8] M.P. Païdoussis, Flutter of conservative systems of pipes conveying incompressible fluid, *Journal of Mechanical Engineering Science* 17 (1975) 19–25.
[9] M. Yoshizawa, H. Nao, E. Hasegawa, Y. Tsujicka, Lateral vibration of a flexible pipe conveying fluid with pulsating flow, *Bulletin of the JSME* 29 (1986) 2243–2250.
[10] Y.L. Zhang, D.G. Gorman, J.M. Reese, Analysis of the vibration of pipes conveying fluid, *Journal of Mechanical Engineering Science* 213 (1999) 849–860.
[11] S.V. Sorokin, A.V. Terentiev, Nonlinear statics and dynamics of a simply supported nonuniform tube conveying an incompressible inviscid fluid, *Journal of Fluids and Structures* 17 (2003) 415–431.
[12] P.J. Holmes, Bifurcations to divergence and flutter in flow-induced oscillations: a finite dimensional analysis, *Journal of Sound and Vibration* 53 (1977) 471–503.
[13] J.M.T. Thompson, T.S. Lunn, Static elastica formulations of a pipe conveying fluid, *Journal of Sound and Vibration* 77 (1981) 127–132.
[14] S. Chucheepsakul, T. Monprapussorn, Divergence instability of variable-arc-length elastica pipes transporting fluid, *Journal of Fluids and Structures* 14 (2000) 895–916.
[15] M. Yoshizawa, H. Nao, E. Hasegawa, Y. Tsujicka, Buckling and postbuckling behavior of a flexible pipe conveying fluid, *Bulletin of the JSME* 28 (1985) 1218–1225.
[16] R.H. Plaut, L.N. Virgin, Use of frequency data to predict buckling, *Journal of Engineering Mechanics* 116 (1990) 2330–2335.
[17] M.A. Langthjem, Y. Sugiyama, Dynamic stability of columns subjected to follower loads: a survey, *Journal of Sound and Vibration* 238 (2000) 809–851.
[18] H. Leipholz, *Direct Variational Methods and Eigenvalue Problems in Engineering*, Noordhoff, Leyden, The Netherlands, 1977.
[19] J. Rousselet, G. Herrmann, Dynamic behavior of continuous cantilevered pipes conveying fluid near critical velocities, *Journal of Applied Mechanics* 48 (1981) 943–947.
[20] S. Wolfram, *The Mathematica Book*, third ed., Cambridge University Press, Cambridge, UK, 1996.
[21] J.E. Flaherty, J.B. Keller, Contact problems involving a buckled elastica, *SIAM Journal on Applied Mathematics* 24 (1973) 215–225.
[22] T.M. Atanackovic, S.S. Simic, On the optimal shape of a Pflüger column, *European Journal of Mechanics A* 18 (1999) 903–913.

[23] L.N. Virgin, R.H. Plaut, Use of frequency data to predict secondary bifurcation, *Journal of Sound and Vibration* 251 (2002) 919–926.
[24] S.J. Britvec, *The Stability of Elastic Systems*, Pergamon, New York, 1973.
[25] L.N. Virgin, R.H. Plaut, Postbuckling and vibration of linearly elastic and softening columns under self-weight, *International Journal of Solids and Structures* 41 (2004) 4989–5001.
[26] K. Huseyin, R.H. Plaut, Transverse vibrations and stability of systems with gyroscopic forces, *Journal of Structural Mechanics* 3 (1974–75) 163–177.
[27] K. Huseyin, *Vibrations and Stability of Multiple Parameter Systems*, Noordhoff, Alphen aan den Rijn, The Netherlands, 1978.